Chalmers Publication Library

Copyright Notice

(Article begins on next page)

On Models, Bounds, and Estimation Algorithms for Time-Varying Phase Noise

M. Reza Khanzadi[†,*], Hani Mehrpouyan[*], Erik Alpman[§], Tommy Svensson[*], Dan Kuylenstierna[†], Thomas Eriksson[*]

[†]Department of Microtechnology and Nanoscience, Microwave Electronics Lab.
[*]Department of Signals and Systems, Communication Systems Group
[†,*]Chalmers University of Technology, Gothenburg, Sweden
[§]Semcon AB, Gothenburg, Sweden
{khanzadi, hanim, tommy.svensson, dan.kuylenstierna, thomase}@chalmers.se, erik.alpman@gmail.com

Abstract—In this paper, a new discrete-time model of phase noise for digital communication systems, based on a comprehensive continuous-time representation of time-varying phase noise is derived and its statistical characteristics are presented. The proposed phase noise model is shown to be more accurate than the classical Wiener model. Next, using the proposed discrete-time model, the *non-data-aided (NDA)* and *decision-directed (DD) maximum-likelihood (ML)* estimators of time-varying phase noise are derived. To evaluate the performance of the proposed estimators, the *Cramér-Rao lower bound (CRLB)* for each estimation approach is derived and by using Monte-Carlo simulations it is shown that the *mean-square error (MSE)* of the proposed estimators converges to the CRLB at moderate *signal-to-noise ratios (SNR)*. Finally, simulation results show that the proposed estimators outperform existing estimation methods as the variance of the phase noise process increases.

I. Introduction

Due to the requirements of high data-rate and spectrum efficient communications, synchronization has gained more attention in the communication community. Since phase noise adversely affects the performance of communication systems, during the last two decades, there have been numerous studies on the estimation and compensation of phase noise in communication systems, e.g., [1]–[8].

Oscillators are an essential part of wireless communication systems and are used to perform frequency and timing synchronization. However, the output of a non-ideal oscillator is not perfectly periodic and suffers from many imperfections that introduce phase noise to communication systems [9]–[13]. In order to effectively estimate and compensate this phase noise, models that accurately capture the characteristics of non-ideal oscillators are required. The classical oscillator phase noise representation is based on the Wiener-Lèvy or random-walk model [5]–[10]. This model is developed according to the Lorentzian portion of the *single-sideband (SSB)* phase noise spectrum, $\mathcal{L}(f)$[1], which has a $1/f^2$ shape [11]. However, empirical measurements of SSB phase noise spectrum of free-running oscillators show that at smaller frequency offsets the phase noise spectrum deviates from the classical model and has a $1/f^3$ shape [13]–[15]. Recent studies show that these two parts of SSB phase noise spectrum are the results of two independent noise processes in the oscillator

circuitry, namely, white and flicker noise [15], [16]. Accordingly, a new model of continuous-time phase noise is proposed in [16], and [15] to explain the shape of SSB phase noise spectrum.

In contrast with the Wiener model which is widely used in the literature, e.g., [5]–[10], the statistical characteristics of this new model in discrete-time domain are not analyzed in detail. Not that knowledge of the statistical characteristics of this new more accurate model can be used to improve the phase noise estimation accuracy in digital communication system which in turn improves the overall system performance.

In [1]–[4], the estimation of constant phase offset using *decision-directed (DD)*[2] and *non-data-aided (NDA)* methods are analyzed in detail. However, very little information on the estimation of time-varying phase noise is presented, and as shown in this paper the proposed estimators' performance deteriorate as the variance of the phase noise process increases. In addition, the phase noise model applied in [4] for deriving the *maximum-likelihood estimator (MLE)* is based on the assumption that the phase fluctuations of each symbol consist of a constant phase plus an *independently and identically distributed (i.i.d)* Gaussian uncertainty. This model is different from the generally accepted Wiener phase noise model, e.g., the model in [5]–[10]. Thus, as shown in this paper the estimator proposed in [4] cannot be used in the case of Wiener phase noise. In addition, the NDA estimators proposed in [4] and [2] require the knowledge of prior and future received signals to estimate the nth symbol's phase noise, which may introduce significant delays in the phase noise estimation process. This estimators are known as offline estimators. Another offline estimator, that can estimate the phase noise of all observation symbols inside a given observation vector, is proposed in [17]. On the other hand, the estimators proposed in this paper are online estimators and only require the N past received symbols while estimating the current symbol's phase noise.

In [6] the *posterior Cramér-Rao bound (PCRB)* [18] and a particle filter based phase noise estimator for the estimation of Wiener phase noise in communication systems are derived. However, the PCRB and estimator in [6] are limited to the case of *Binary Phase Shift Keying (BPSK)* modulation. Moreover, the PCRB in [6] is derived for the case of Wiener phase noise and hence is not valid for the new model proposed in this

---

[1]SSB phase noise spectrum, $\mathcal{L}(f)$, is defined as the power spectral density of the total oscillatory signal around the central oscillation frequency, f_c, expressed as a function of the offset frequency f from f_c, and normalized with the total power of the oscillator's signal [10].

[2]Information on prior data symbols are used to estimate the nth symbol's phase noise or phase fluctuation.

paper in which the phase variation during each time instant is correlated with the phase variations during the past time instants (see Sec. III). In this paper, the PCRB of [6] is compared with the proposed *Cramér-Rao lower bounds (CRLBs)* for the case of BPSK and it is shown that two bounds coincide under most practical scenarios of interest. The *Bayesian Cramér-Rao bound (BCRB)* [19] for evaluation of the estimation performance in the case of Wiener phase noise is proposed in [8]. This study is also limited to the case of BPSK modulation and is only focused on the NDA scenario. No estimator is designed and extending the result to more complex modulation schemes is very difficult.

In [7] the effect of imperfect phase noise estimation on the bit error probability of *quadratic phase-shift keying (QPSK)* modulated signals is investigated. However, the results are limited and the performance of the proposed estimator is not evaluated. Other phase noise estimation methods, such as iterative methods are also presented in the literature, e.g., [20]–[22]. These iterative algorithms are usually complex to implement.

The contributions of this paper can be summarized as follows:
• A new discrete-time model of the phase noise is proposed which is a generalized version of the discrete-time Wiener model. This model resembles the measured SSB phase noise spectrum of a free-running oscillator more closely and takes into account the effect of both $1/f^2$ and $1/f^3$-shaped portions of the SSB phase noise spectrum. The statistical characteristics of the new model are also derived.
• Based on the proposed model, new NDA and DD MLEs and CRLBs for estimation of the phase noise in *M*-ary PSK modulated signals are derived in closed form. It is also shown that the derived bounds and estimators are applicable to the Wiener phase noise.

In Sec. II, a system model for a point-to-point communication system using *M*-ary PSK modulation is introduced. In Sec.III, first, a continuous-time phase noise model in [15], [16] is briefly studied. Then, the mentioned discrete-time model of the phase noise is proposed based on this model. In Sec.IV, based on the proposed model, new NDA and DD MLEs and CRLBs for estimation of phase noise are derived. In Sec. V, the performance of the derived estimators, for both the proposed phase noise model and the Wiener model, are compared against the CRLB and existing estimators and bounds in the literature.

Notations: italic letters (x) are scalar variables, bold letters $(\mathbf{x})$ are vectors, bold upper case letters $(\mathbf{X})$ are matrices, $(X^{a,b})$ denotes the $(a,b)th$ entry of matrix $\mathbf{X}$, $\mathbb{E}[\cdot]$ denotes the statistical expectation, $\Re(\cdot)$, $\Im(\cdot)$, and $\arg(\cdot)$ are real part, imaginary part, and angle of complex values, and $(\cdot)^*$, $(\cdot)^T$, and $(\cdot)^H$ are conjugate, transpose, and conjugate transpose, respectively.

II. SYSTEM MODEL

Fig. 1 depicts the block diagram corresponding to the complex baseband representation of the considered communication system. The received signal, r_k, can be written as

$$r_k = e^{j\phi_k} s_k + w_k, \tag{1}$$

where s_k is the *M*-ary PSK modulated symbol transmitted at time instant k, $e^{j\phi_k}$ represents the phasor of ϕ_k, which is the unwanted
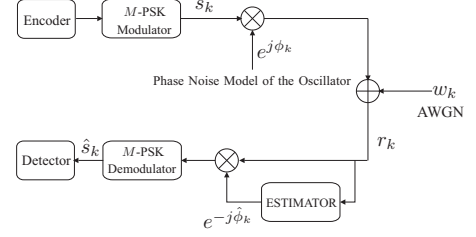

Fig. 1: System Model.

phase fluctuation of the kth received symbol, r_k, and w_k is the zero-mean complex *additive white Gaussian noise (AWGN)* with variance σ_w^2. The source and statistical model of ϕ_k are discussed in detail in Sec. III. Throughout this paper it is assumed that the timing offset and channel gain have been estimated and compensated which is in line with the assumptions in [1]–[8]. As shown in Fig. 1, the received signal is passed through a phase estimator and the estimated phase, $\hat{\phi}_k$, is used to de-rotate the received signal before demodulation.

III. PHASE NOISE MODEL

In this section the phase noise model in [15], [16], which closely resembles measurement results for a free-running oscillator, is briefly introduced. Then we derive the statistical properties of the discrete-time version of this model, given that it is of more interest in digital communication systems.

A. Overview

As illustrated in Fig. 2 and shown in [15], [16], far from the central carrier frequency, f_c, the oscillator SSB phase noise spectrum has a $1/f^2$ shape. However, as we move closer to f_c, the oscillator SSB phase noise spectrum changes to a $1/f^3$ shape, and for further lower frequency offsets a Gaussian shape of SSB phase noise spectrum can be observed. The classical Wiener phase noise model is motivated by the $1/f^2$ shape portion of the oscillator's spectrum, also known as Lorentzian spectrum [5]. However, the $1/f^3$ and Gaussian portions of the oscillator's SSB phase noise spectrum need to be taken into consideration to find a comprehensive phase noise model.

As shown in [15], [16], the output of a noisy oscillator is given by $\zeta(t) = \cos(2\pi f_c t + \phi(t))$, where $\phi(t)$ is the phase fluctuations that is modeled as a real *random process (RP)*. In the continuous-time domain, the phase fluctuation can be expressed as

$$\phi(t) = \int_0^t \Omega(u)\, \mathrm{d}u, \tag{2}$$

where $\Omega(t)$ is the frequency perturbation, which is a result of different parameters such as thermal noise of circuit elements, noise of transistors, fluctuations in the tuning voltage of *voltage controlled oscillators (VCO)*, etc. [23], [24]. In practice, $\Omega(t)$ is assumed to be a stationary zero-mean Gaussian RP and can be white or colored depending on the source of the noise [11], [15], [24]. As shown in [11], [15], [16] the $1/f^2$-shaped portion is produced by white frequency noise, $\Omega_{\text{white}}(t)$, while the $1/f^3$-shaped plus the Gaussian-shaped portions are due to flicker noise, $\Omega_{\text{flicker}}(t)$, with an approximate *power spectral density (PSD)* equal to $1/f^{(1-\nu)}$. Note that, ν has a small value ($0 < \nu < 1$) and is used to ensure the stationarity of $\Omega_{\text{flicker}}(t)$ [15], [16]. Finally,

the total phase fluctuation, $\phi(t)$, can be written as

$$\phi(t) = \phi_{\text{white}}(t) + \phi_{\text{flicker}}(t), \qquad (3)$$

where $\phi_{\text{white}}(t)$ and $\phi_{\text{flicker}}(t)$ are two independent phase noise processes, which are produced by $\Omega_{\text{white}}(t)$ and $\Omega_{\text{flicker}}(t)$, respectively.

Using (2), the phase noise variation caused by the phase noise process during the time interval τ is defined as

$$\xi(t, \tau) = \phi(t) - \phi(t - \tau) = \int_{t-\tau}^{t} \Omega(u) \, \mathrm{d}u, \qquad (4)$$

where $\xi(t, \tau)$ denotes the phase noise innovation and according to the properties of $\Omega(t)$, it is a zero-mean Gaussian RP. Note that the variance and correlation properties of $\xi(t, \tau)$ are dependent on the properties of $\Omega(t)$.

B. A New Discrete-Time Phase Noise Model

In this section, a new discrete-time phase noise model, consisting of both $\phi_{\text{white}}(t)$ and $\phi_{\text{flicker}}(t)$ is proposed, and its statistical properties are derived.

According to (4) and considering a sampling time T_s, the phase innovation between two consecutive samples can be written as

$$\Delta_n \triangleq \xi(nT_s, T_s) = \phi(nT_s) - \phi(nT_s - T_s) = \int_{(n-1)T_s}^{nT_s} \Omega(u) \, \mathrm{d}u, \qquad (5)$$

where Δ_n is the discrete version of $\xi(t, \tau)$. Using (5), the phase fluctuation of the nth sample, $\phi_n \triangleq \phi(nT_s)$, can be expressed as

$$\phi_n = \phi_{n-1} + \Delta_n. \qquad (6)$$

According to (3), the total phase noise innovation can be written as addition of two independent phase noise innovations

$$\Delta_n = \Delta_{\text{white},n} + \Delta_{\text{flicker},n}, \qquad (7)$$

where $\Delta_{\text{white},n}$ and $\Delta_{\text{flicker},n}$ denote the phase noise innovation corresponding to $\Omega_{\text{white}}(t)$ and $\Omega_{\text{flicker}}(t)$, respectively. Note that for the Wiener model, only the white phase noise innovation, $\Delta_{\text{white},n}$, is considered and $\Delta_{\text{flicker},n}$ is usually neglected despite its important effect on the final phase noise process.

Based on the above assumptions, the autocorrelation function of Δ_n can be calculated as

$$R_\Delta(l) = \mathbb{E}\left[\Delta_n \Delta_{n+l}\right] \qquad (8)$$

$$= \mathbb{E}\left[\int_{(n-1)T_s}^{nT_s} \int_{(n+l-1)T_s}^{(n+l)T_s} \Omega(u)\Omega(v)\mathrm{d}u\mathrm{d}v\right]$$

$$= \int_{(n-1)T_s}^{nT_s} \int_{(n+l-1)T_s}^{(n+l)T_s} R_\Omega(u - v)\mathrm{d}u\mathrm{d}v,$$

where $R_\Omega(u - v)$ denotes the autocorrelation function of $\Omega(t)$. Using the Fourier transform of $R_\Omega(u - v)$, $R_\Delta(l)$ can be written as

$$R_\Delta(l) = \int_{-\infty}^{\infty} \Bigg\{ S_\Omega(f) \qquad (9)$$
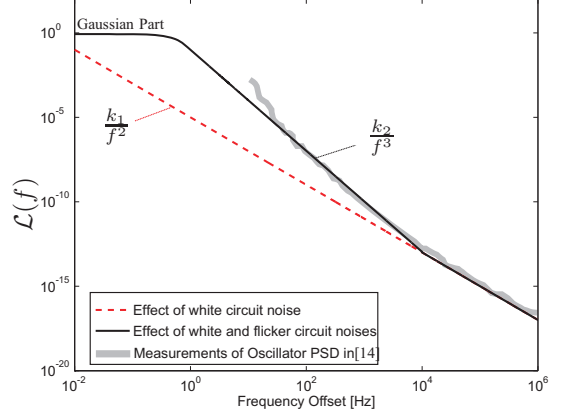$$\int_{(n-1)T_s}^{nT_s} \int_{(n+l-1)T_s}^{(n+l)T_s} e^{j2\pi f(u-v)}\mathrm{d}u\mathrm{d}v \Bigg\}\mathrm{d}f,$$

Fig. 2: $\mathcal{L}(f)$ of a free-running oscillator. $k_1 = 4 \times 10^{-4}, k_2 = 0.1, \nu = 0.01$, if $T_s = 10^{-6} \Rightarrow \sigma^2_{\Delta_{\text{white}}} = 4 \times 10^{-10}, \sigma^2_{\Delta_{\text{flicker}}} = 1.7 \times 10^{-5}$.

where $S_\Omega(f)$ denotes the PSD of $\Omega(t)$. By evaluating the two internal integrals with respect to u and v and carrying out straightforward algebraic manipulations $R_\Delta(l)$ can be found as

$$R_\Delta(l) = 2\int_0^\infty S_\Omega(f) \frac{\cos(2\pi f l T_s)(1 - \cos(2\pi T_s))}{(2\pi f)^2} \mathrm{d}f. \qquad (10)$$

The autocorrelation of $\Delta_{\text{white},n}$ can be found by using (10) and assuming a constant PSD, i.e., $S_{\Omega_{\text{white}}}(f) = K_1$, such that

$$R_{\Delta_{\text{white}}}(l) = \begin{cases} \sigma^2_{\Delta_{\text{white}}} = \frac{K_1 T_s}{2} & \text{if } l = 0 \\ 0 & \text{if } l \neq 0 \end{cases}, \qquad (11)$$

where $\sigma^2_{\Delta_{\text{white}}}$ is the variance of $\Delta_{\text{white},n}$, which is a linear function of the sampling time T_s. For this case, the phase noise process $\phi_{\text{white}}(t)$ is a special case of discrete *fractional Brownian motion (fBm)* [25] with uncorrelated innovations also known as a Wiener Process.

Using (10) and $S_{\Omega_{\text{flicker}}}(f) = \frac{K_2}{|f|^{1-\nu}}$, the autocorrelation function of $\Delta_{\text{flicker},n}$ can be determined as

$$R_{\Delta_{\text{flicker}}}(l) = \frac{\sigma^2_{\Delta_{\text{flicker}}}}{2}\left(|l-1|^{2-\nu} - 2|l|^{2-\nu} + |l+1|^{2-\nu}\right), \qquad (12)$$

where $\sigma^2_{\Delta_{\text{flicker}}}$ is the variance, which is given by

$$\sigma^2_{\Delta_{\text{flicker}}} = \frac{-K_2\pi}{(2\pi)^\nu \Gamma(3-\nu)\cos(\frac{(3-\nu)\pi}{2})}T_s^{2-\nu}. \qquad (13)$$

Note that the phase noise process, $\phi_{\text{flicker}}(t)$, with the autocorrelation function defined by (12) for its innovations, is an fBm [25], where the variance of the innovations is approximately proportional to T_s^2.

Finally, according to (7), the autocorrelation function of the total phase noise innovation, Δ_n, is determined as

$$R_\Delta(l) = R_{\Delta_{\text{white}}}(l) + R_{\Delta_{\text{flicker}}}(l), \qquad (14)$$

where $R_{\Delta_{\text{white}}}(l)$, and $R_{\Delta_{\text{flicker}}}(l)$ are defined in (11), and (12), respectively.

IV. ESTIMATION OF TIME-VARYING PHASE NOISE

In the following subsections, four algorithms for estimation of the kth received symbol's phase noise, ϕ_k, are derived. In addition, a CRLB is derived for each case to evaluate the performance of each estimator. The proposed algorithms are based

on *non-data-aided (NDA)* and *decision-directed (DD)* methods. In each method two different schemes, based on the *high-SNR* and *slow-varying phase noise* assumptions are implemented.

According to the phase noise model in (6), (7) and Fig. 3, the phase noise of the $(k-i)$th received symbol is determined as

$$\phi_{k-i} = (\phi_k - \sum_{m=0}^{i-1} \Delta_m). \qquad (15)$$

Using (15) and the system model developed in Sec.II, the $(k-i)$th received symbol, r_{k-i}, can be written as

$$r_{k-i} = s_{k-i} e^{j(\phi_k - \sum_{m=0}^{i-1} \Delta_m)} + w_{k-i}. \qquad (16)$$

Note that all statistical properties of the random phase noise, ϕ_k, is translated to the model in (15) and (16). Thus, hereinafter, ϕ_k is assumed as an unknown deterministic parameter over the observation sequence.

A. Non-Data-Aided Estimator

In order to remove the data dependency, the received signal can be passed through a nonlinear function [2]. Here, the approach proposed in [4] is used, where the received *M*-ary PSK symbols are raised to the power of M. Based on this approach, (16) can be rewritten as

$$r_{k-i}^M = (s_{k-i} e^{j(\phi_k - \sum_{m=0}^{i-1} \Delta_m)} + w_{k-i})^M. \qquad (17)$$

Using the binomial theorem, r_{k-i}^M can be rewritten as

$$r_{k-i}^M = \sum_{l=0}^{M} \binom{M}{l} (s_{k-i} e^{j(\phi_k - \sum_{m=0}^{i-1} \Delta_m)})^{M-l} w_{k-i}^l \qquad (18)$$

$$= \binom{M}{0} (s_{k-i} e^{j(\phi_k - \sum_{m=0}^{i-1} \Delta_m)})^M w_{k-i}^0$$

$$+ \binom{M}{1} (s_{k-i} e^{j(\phi_k - \sum_{m=0}^{i-1} \Delta_m)})^{M-1} w_{k-i}^1$$

$$+ \binom{M}{2} (s_{k-i} e^{j(\phi_k - \sum_{m=0}^{i-1} \Delta_m)})^{M-2} w_{k-i}^2 + \cdots.$$

Assuming that the signal power is much larger than the noise w_{k-i}, the remaining terms after the second term in (18) can be neglected. By defining the *M*-ary PSK modulated symbol $s_k = \sqrt{E_s} e^{j(\frac{2\pi L_k}{M})}$, where E_s denotes the signal energy and $L_k \in \{1, \ldots, M\}$ is the index of transmitted message, s_k^M, can be determined as

$$s_k^M = E_s^{\frac{M}{2}} e^{j(\frac{2\pi L_k}{M})M} = E_s^{\frac{M}{2}}. \qquad (19)$$

Using (19) and by keeping only the first two terms of (18), $\dot{r}_{k-i} \triangleq r_{k-i}^M$ can be rewritten as

$$\dot{r}_{k-i} = E_s^{\frac{M}{2}} e^{jM(\phi_k - \sum_{m=0}^{i-1} \Delta_m)} \qquad (20)$$

$$+ \underbrace{M E_s^{\frac{M-1}{2}} e^{j((M-1)(\phi_k - \sum_{m=0}^{i-1} \Delta_m) + \arg(s_{k-i}^{M-1}))} w_{k-i}}_{\triangleq \dot{w}_{k-i}},$$

where $\dot{w}_{k-i}$, a rotated and scaled version of w_{k-i}, is still a zero-mean complex Gaussian *random variable (RV)* with variance $\sigma_{\dot{w}}^2 = M^2 E_s^{(M-1)} \sigma_w^2$. This is based on the assumption of circularity on the observation noise.

$$\begin{array}{c|c|c|c|c|c}
\mathbf{r}: & r_{k-N+1} & \cdots & r_{k-2} & r_{k-1} & r_k \\
\hline
\phi: & \phi_k - \sum_{m=0}^{N-2} \Delta_m & \cdots & \phi_k - \Delta_1 - \Delta_2 & \phi_k - \Delta_1 & \phi_k
\end{array}$$

N symbols

Fig. 3: Vector of N received symbols and its corresponding phase fluctuation vector.

1) High-SNR: By defining $\ddot{w}_{k-i} \triangleq \dot{w}_{k-i} e^{-jM(\phi_k - \sum_{m=0}^{i-1} \Delta_m)}$ (20) is rewritten as

$$\dot{r}_{k-i} = (E_s^{\frac{M}{2}} + \ddot{w}_{k-i}) e^{jM(\phi_k - \sum_{m=0}^{i-1} \Delta_m)} \qquad (21)$$

$$= |E_s^{\frac{M}{2}} + \ddot{w}_{k-i}| e^{j(\arg(E_s^{\frac{M}{2}} + \ddot{w}_{k-i}) + M(\phi_k - \sum_{m=0}^{i-1} \Delta_m))},$$

where $\ddot{w}_{k-i}$ is the rotated version of $\dot{w}_{k-i}$ with variance $\sigma_{\ddot{w}}^2 = \sigma_{\dot{w}}^2$. Next, note that

$$\arg(E_s^{\frac{M}{2}} + \ddot{w}_{k-i}) = \tan^{-1}\left(\frac{\Im(\ddot{w}_{k-i})}{E_s^{\frac{M}{2}} + \Re(\ddot{w}_{k-i})}\right). \qquad (22)$$

At high SNR, since $\frac{\Im(\ddot{w}_{k-i})}{E_s^{\frac{M}{2}}}$ is small and $\tan^{-1}(x) \approx x$ for small x, (22) can be rewritten as

$$\arg(E_s^{\frac{M}{2}} + \ddot{w}_{k-i}) \approx \frac{\Im(\ddot{w}_{k-i})}{E_s^{\frac{M}{2}}} \triangleq \dddot{w}_{k-i}. \qquad (23)$$

The accuracy of this approximation is evaluated in Sec. V by means of numerical simulations. The SNR range in which *High-SNR* assumption is valid is discussed in Remark 1. Using (21), (22), and (23), $\arg(\dot{r}_{k-i})$ can be written as

$$a_{k-i} \triangleq \arg(\dot{r}_{k-i}) = M\phi_k - M\sum_{m=0}^{i-1} \Delta_m + \dddot{w}_{k-i}, \qquad (24)$$

where $\dddot{w}_{k-i}$, a zero-mean real Gaussian RV with variance $\sigma_{\dddot{w}}^2 = \frac{\sigma_{\ddot{w}}^2}{2E_s^M}$, is defined in (23). Since summation of zero-mean real Gaussian RVs is a real Gaussian RV, a_{k-i} is also a real Gaussian RV. Therefore, the vector $\mathbf{a} \triangleq [a_{k-N+1}, \ldots, a_k]^T$ has an N−variate Gaussian distribution given by

$$f_{\mathbf{a}|\phi_k}(\mathbf{a}|\phi_k) = \frac{1}{\sqrt{((2\pi)^N \det(\mathbf{C}_a))}} e^{[-\frac{1}{2}(\mathbf{a}-\mathbf{m}_a)^T \mathbf{C}_a^{-1}(\mathbf{a}-\mathbf{m}_a)]}, \qquad (25)$$

where $\mathbf{m}_a = M\phi_k \mathbf{1}^{N\times 1}$ and $\mathbf{C}_a^{N\times N}$ denote the mean and covariance of $\mathbf{a}$, respectively and $\mathbf{1} \triangleq [1, 1, \ldots, 1]^T$. The elements of the covariance matrix $\mathbf{C}_a^{N\times N}$ can be determined as

$$C_a^{x+1,y+1} = \mathbb{E}[(a_{k-x} - \mathbb{E}[a_{k-x}])(a_{k-y} - \mathbb{E}[a_{k-y}])] \qquad (26)$$

$$= \mathbb{E}[(a_{k-x} - M\phi_k)(a_{k-y} - M\phi_k)]$$

$$= \mathbb{E}[(-M\sum_{n=0}^{x-1} \Delta_n + \dddot{w}_{k-x})(-M\sum_{m=0}^{y-1} \Delta_m + \dddot{w}_{k-})]$$

$$= M^2 \sum_{m=0}^{x-1} \sum_{n=0}^{y-1} \mathbb{E}[\Delta_m \Delta_n] + \mathbb{E}[\dddot{w}_{k-x} \dddot{w}_{k-y}]$$

$$= M^2 \sum_{m=0}^{x-1} \sum_{n=0}^{y-1} (R_{\Delta_{\text{white}}}(m-n) + R_{\Delta_{\text{flicker}}}(m-n))$$

$$+ \delta(x-y) \frac{M^2 \sigma_w^2}{2E_s},$$

where $x, y \in \{0, \ldots, N-1\}$. The *log-likelihood function (LLF)* of ϕ_k, up to an additive constant is given by

$$L(\phi_k) = \ln(f_{\mathbf{a}|\phi_k}) = -\frac{1}{2}(\mathbf{a} - \mathbf{m}_a)^T \mathbf{C}_a^{-1}(\mathbf{a} - \mathbf{m}_a). \quad (27)$$

In order to find the MLE of ϕ_k, $\hat{\phi}_k$, the LLF in (27) needs to be maximized, where the derivative of $L(\phi_k)$ with respect to ϕ_k is determined as

$$\frac{\partial L(\phi_k)}{\partial \phi_k} = \frac{1}{2}[M\mathbf{a}^T\mathbf{C}_a^{-1}\mathbf{1} + M\mathbf{1}^T\mathbf{C}_a^{-1}\mathbf{a} - 2M^2\phi_k\mathbf{1}^T\mathbf{C}_a^{-1}\mathbf{1}]. \quad (28)$$

By setting (28) equal to zero and by carrying out straightforward algebraic manipulations, the MLE for ϕ_k can be derived as

$$\hat{\phi}_{k(\text{NDA}_h)} = \frac{\mathbf{1}^T\mathbf{C}_a^{-1}\mathbf{a}}{M(\mathbf{1}^T\mathbf{C}_a^{-1}\mathbf{1})}. \quad (29)$$

Given that the *Cramér-Rao lower bound (CRLB)* is defined as [26]

$$\text{CRLB} = \left(\mathbb{E}\left[-\frac{\partial^2 L(\phi_k)}{\partial \phi_k^2}\right]\right)^{-1}, \quad (30)$$

the CRLB for the estimation of ϕ_k using the *high-SNR* assumption, $\text{CRLB}_{(\text{NDA}_h)}$, is calculated as

$$\text{CRLB}_{(\text{NDA}_h)} = \frac{1}{M^2(\mathbf{1}^T\mathbf{C}_a^{-1}\mathbf{1})}. \quad (31)$$

2) Slow-Varying Phase Noise: The Taylor series expansion of e^x for small values of x can be approximated by $e^x \approx 1 + x$. Based on the assumption of *slow-varying phase noise*, the sum of the phase innovations $M\sum_{m=0}^{i-1}\Delta_m$ can be considered to be small. Thus, $e^{-jM\sum_{m=0}^{i-1}\Delta_m}$ can be approximated by

$$e^{-jM\sum_{m=0}^{i-1}\Delta_m} \approx 1 - jM\sum_{m=0}^{i-1}\Delta_m. \quad (32)$$

The *slow-varying phase noise* assumption and approximation in (32) is used and verified in the literature, e.g., [5], [7], [27]–[29]. The results in Sec. V, where the performance of the estimator proposed in this subsection is compared against the CRLB, also validate this assumption (see also Remark 2). Using (32), (20) can be rewritten as

$$\dot{r}_{k-i}^M = E_s^{\frac{M}{2}}e^{jM\phi_k}(1 - jM\sum_{m=0}^{i-1}\Delta_m) + \dot{w}_{k-i} \quad (33)$$

$$= E_s^{\frac{M}{2}}e^{jM\phi_k} - jME_s^{\frac{M}{2}}e^{jM\phi_k}\sum_{m=0}^{i-1}\Delta_m + \dot{w}_{k-i}.$$

Given that Δ_m and $\dot{w}_{k-i}$ are Gaussian RVs and based on (33) the vector $\dot{\mathbf{r}} \triangleq [\dot{r}_{k-N+1}^M, \ldots, \dot{r}_k^M]^T$ has an $N-$variate complex Gaussian distribution given by

$$f_{\dot{\mathbf{r}}|\phi_k}(\dot{\mathbf{r}}|\phi_k) = \frac{1}{(\pi)^N \det(\mathbf{C}_{\dot{r}})}e^{[-(\dot{\mathbf{r}}-\mathbf{m}_{\dot{r}})^H\mathbf{C}_{\dot{r}}^{-1}(\dot{\mathbf{r}}-\mathbf{m}_{\dot{r}})]}, \quad (34)$$

where $\mathbf{m}_{\dot{r}} = E_s^{\frac{M}{2}}e^{jM\phi_k}\mathbf{1}^{N\times 1}$ is the mean vector. Taking the same approach as (26), elements of the covariance matrix $\mathbf{C}_{\dot{r}}^{N\times N}$ can be determined as

$$C_{\dot{r}}^{x+1,y+1} = M^2E_s^M\sum_{m=0}^{x-1}\sum_{n=0}^{y-1}(R_{\Delta_{\text{white}}}(m-n) + R_{\Delta_{\text{flicker}}}(m-n))$$
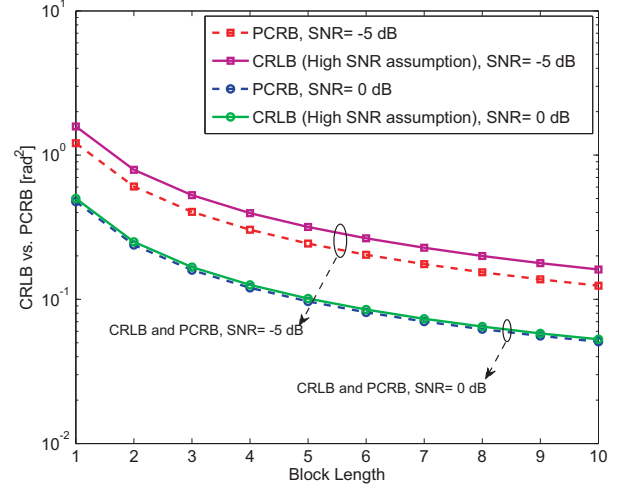$$+ M^2E_s^{M-1}\delta(x-y)\sigma_w^2. \quad (35)$$

Fig. 4: Comparing the proposed CRLB of *NDA method using high-SNR assumption* vs. PCRB in [6] for different SNR values and different observation block lengths in BPSK modulation case, (Wiener model $\sigma_{\Delta_{\text{white}}}^2 = 10^{-3}$ and $\sigma_{\Delta_{\text{flicker}}}^2 = 0$).

In order to find the MLE for ϕ_k, first the LLF, up to an additive constant, is determined as

$$L(\phi_k) = \ln(f_{\dot{\mathbf{r}}|\phi_k}) = -(\dot{\mathbf{r}} - \mathbf{m}_{\dot{r}})^H\mathbf{C}_{\dot{r}}^{-1}(\dot{\mathbf{r}} - \mathbf{m}_{\dot{r}}). \quad (36)$$

The derivative of LLF with respect to ϕ_k can be calculated as

$$\frac{\partial L(\phi_k)}{\partial \phi_k} = jME_s^{\frac{M}{2}}[e^{jM\phi_k}\dot{\mathbf{r}}^H\mathbf{C}_{\dot{r}}^{-1}\mathbf{1} - e^{-jM\phi_k}\mathbf{1}^T\mathbf{C}_{\dot{r}}^{-1}\dot{\mathbf{r}}]. \quad (37)$$

Finally, by setting $\frac{\partial L(\phi_k)}{\partial \phi_k}$ in (37) equal to zero the MLE of ϕ_k is given by

$$\hat{\phi}_{k(\text{NDA}_s)} = \frac{1}{M}\tan^{-1}\frac{\Im(\mathbf{1}^T\mathbf{C}_{\dot{r}}^{-1}\dot{\mathbf{r}})}{\Re(\mathbf{1}^T\mathbf{C}_{\dot{r}}^{-1}\dot{\mathbf{r}})}. \quad (38)$$

Using (30), the CRLB for estimation of ϕ_k using the *slow-varying phase noise* assumption, $\text{CRLB}_{(\text{NDA}_s)}$, is given by

$$\text{CRLB}_{(\text{NDA}_s)} = \frac{1}{2M^2E_s^M(\mathbf{1}^T\mathbf{C}_{\dot{r}}^{-1}\mathbf{1})}. \quad (39)$$

The following remarks are in order:

Remark 1: In Fig. 4, the proposed CRLB of the NDA scheme, using the *High-SNR* assumption, is compared with the PCRB in [6] for the case of BPSK modulation. This figure shows that the *High-SNR* assumption is valid for a large range of SNR values. It can be seen that the proposed CRLB is close to the PCRB of [6] even for the low SNR values, e.g., -5 dB, and 0 dB.

Remark 2: Fig. 5 compares the proposed CRLB of the NDA method using the *slow-varying phase* noise assumption, and the PCRB introduced in [6]. As illustrated in this figure, increasing the observation block length results in a better estimation performance. Moreover, it validates the slow-varying phase noise assumption for the given phase noise innovation variances. According to the empirical measurements of the phase noise in the literature, e.g., [12], 10^{-3} rad^2 or 10^{-4} rad^2 are reasonable assumptions for the variance of the phase noise innovations for typical free running oscillators. Fig. 5 shows that the proposed CRLB bound is close to the PCRB of [6] and validates the *slow-varying phase noise* assumption in this paper.
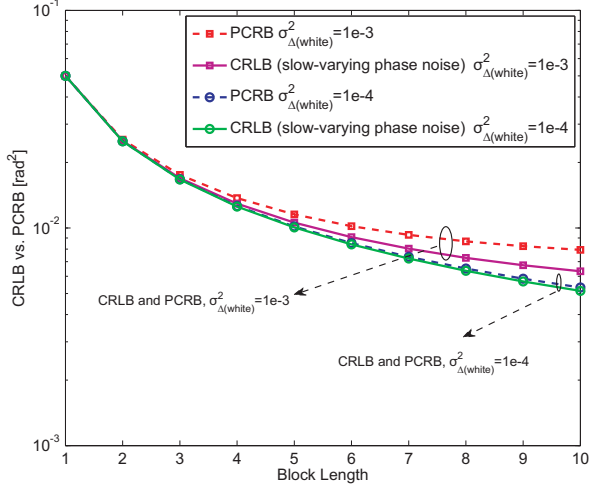
Fig. 5: Comparing the proposed CRLB of *NDA method using slow-varying phase noise assumption* vs. PCRB in [6] for different phase noise innovation variances and different observation block lengths in BPSK modulation case, SNR=10 dB, (Wiener model $\sigma^2_{\Delta_{\text{flicker}}} = 0$).

Remark 3: Although the above approach removes the data dependency, it results in a phase ambiguity of $2\pi/M$. In practice training sequences and pilots or differential modulation can be used to solve this problem [4].

Remark 4: Given that the process of removing data dependency in (18) amplifies the AWGN by a factor of M, where M is the constellation size, the proposed NDA estimators' performance degrades as M increases.

B. Decision-Directed Estimator

The DD scenario is of interest given that in most communication systems training sequences or pilot signals are used to facilitate accurate and efficient estimation of synchronization parameters. In this paper the DD scenario refers to the scenario where the kth symbol's phase noise is estimated while assuming that the transmitted symbols prior to the kth symbol are known.

After multiplying r_{k-i} by the conjugate of the known transmitted symbol, s^*_{k-i}, one obtains

$$\tilde{r}_{k-i} \triangleq s^*_{k-i} r_{k-i} = E_s e^{j(\phi_k - \sum_{m=0}^{i-1} \Delta_m)} + \dot{w}_{k-i}, \quad (40)$$

where $\dot{w}_{k-i}$ is a zero-mean complex Gaussian RV with variance $\sigma^2_{\dot{w}} = E_s \sigma^2_w$. Similar to the NDA method, two estimators based on the *high-SNR* and *slow-varying phase noise* assumptions are derived in the following subsections.

1) High-SNR: Using the same steps as the ones outlined in Sec.IV-A, $\tilde{r}_{k-i}$ can be rewritten as

$$\tilde{r}_{k-i} = |E_s + \ddot{w}_{k-i}| e^{j(\phi_k - \sum_{m=0}^{i-1} \Delta_m + \ddot{w}_{k-i})}, \quad (41)$$

where $\ddot{w}_{k-i}$, is a rotated version of $\dot{w}_{k-i}$, and $\ddot{w}_{k-i}$ is a real Gaussian RV with variance $\sigma^2_{\ddot{w}} = \frac{\sigma^2_w}{2E_s}$. From (41), it is clear that the useful information for the estimation of ϕ_k is the angle of $\tilde{r}_{k-i}$. Let us define $\tilde{a}_{k-i} \triangleq \arg(\tilde{r}_{k-i})$ and $\tilde{\mathbf{a}} \triangleq [\tilde{a}_{k-N}, \ldots, \tilde{a}_{k-1}]^T$, where $\tilde{\mathbf{a}}$ has an N-variate Gaussian distribution similar to that of (25). The mean vector and covariance matrix of $\tilde{\mathbf{a}}$ are given by $\mathbf{m}_{\tilde{a}} = \phi_k \mathbf{1}^{N \times 1}$ and $\mathbf{C}^{N \times N}_{\tilde{a}}$, respectively. Using similar steps as

(26), $\mathbf{C}^{N \times N}_{\tilde{a}}$ can be calculated as

$$C^{x,y}_{\tilde{a}} = \sum_{m=0}^{x-1} \sum_{n=0}^{y-1} (R_{\Delta_{\text{white}}}(m-n) + R_{\Delta_{\text{flicker}}}(m-n)) \quad (42)$$
$$+ \delta(x-y)\frac{\sigma^2_w}{2E_s},$$

where $x, y \in \{1, \ldots, N\}$. Analogous to Sec. IV-A, the MLE and CRLB can be determined as

$$\hat{\phi}_{k(\text{DD}_\text{h})} = \frac{\mathbf{1}^T \mathbf{C}^{-1}_{\tilde{a}} \tilde{\mathbf{a}}}{\mathbf{1}^T \mathbf{C}^{-1}_{\tilde{a}} \mathbf{1}}, \quad \text{CRLB}_{(\text{DD}_\text{h})} = \frac{1}{\mathbf{1}^T \mathbf{C}^{-1}_{\tilde{a}} \mathbf{1}}. \quad (43)$$

2) Slow-Varying Phase Noise: Based on the assumption that $\sum_{m=0}^{i-1} \Delta_m$ has a small value, (40) can be rewritten as

$$\tilde{r}_{k-i} = E_s e^{j\phi_k} (1 - j \sum_{m=0}^{i-1} \Delta_m) + \dot{w}_{k-i} \quad (44)$$

$$= E_s e^{j\phi_k} - j E_s e^{j\phi_k} \sum_{m=0}^{i-1} \Delta_m + \dot{w}_{k-i}.$$

According to (44), the observation vector $\tilde{\mathbf{r}} \triangleq [\tilde{r}_{k-N}, \ldots, \tilde{r}_{k-1}]^T$ has an N-variate complex Gaussian distribution in the form of (34) with mean vector $\mathbf{m}_{\tilde{r}} = E_s e^{j\phi_k} \mathbf{1}^{N \times 1}$. Similar to (26), the elements of the covariance matrix $\mathbf{C}^{N \times N}_{\tilde{r}}$ are determined as

$$C^{x,y}_{\tilde{r}} = E_s^2 \sum_{m=0}^{x-1} \sum_{n=0}^{y-1} (R_{\Delta_{\text{white}}}(m-n) + R_{\Delta_{\text{flicker}}}(m-n)) \quad (45)$$
$$+ E_s \delta(x-y)\sigma^2_w,$$

where $x, y \in \{1, \ldots, N\}$. The MLE and CRLB for this scenario can be determined as

$$\hat{\phi}_{k(\text{DD}_\text{s})} = \tan^{-1} \frac{\Im(\mathbf{1}^T \mathbf{C}^{-1}_{\tilde{r}} \tilde{\mathbf{r}})}{\Re(\mathbf{1}^T \mathbf{C}^{-1}_{\tilde{r}} \tilde{\mathbf{r}})}, \quad \text{CRLB}_{(\text{DD}_\text{s})} = \frac{1}{2E_s^2 \mathbf{1}^T \mathbf{C}^{-1}_{\tilde{r}} \mathbf{1}}. \quad (46)$$

V. SIMULATION AND RESULTS

In this section, the performance of the proposed MLEs is evaluated by Monte-Carlo simulations and the results are compared to the derived CRLBs for both the Wiener and the proposed fBm models. In addition, the phase noise estimator in [4] is simulated and its performance is compared to the proposed MLEs.

The output range of the derived estimators are limited due to the use of $\tan^{-1}(\cdot)$ operator. To improve the estimation range, an unwrapping algorithm similar to that of [4] is applied. In [4], phase noise estimates for prior symbols are used in combination with the phase noise variance to unwrap the estimate for the current symbol.

Fig. 6 compares the CRLBs of the NDA method using *slow-varying phase noise* approach for different phase noise variances and SNRs. As illustrated, at low-to-medium SNRs, the higher the phase noise innovation variance the higher is the CRLB for the estimation of the phase noise. However, at high SNRs, the performance of the proposed NDA estimator for different phase noise variances converges to the same value.

In Fig. 7 the performances of the NDA estimators based on the *high-SNR* and *slow-varying phase noise* assumptions are compared against one another. As illustrated, compared to the *high-SNR* approach, the *mean-square error (MSE)* of the proposed
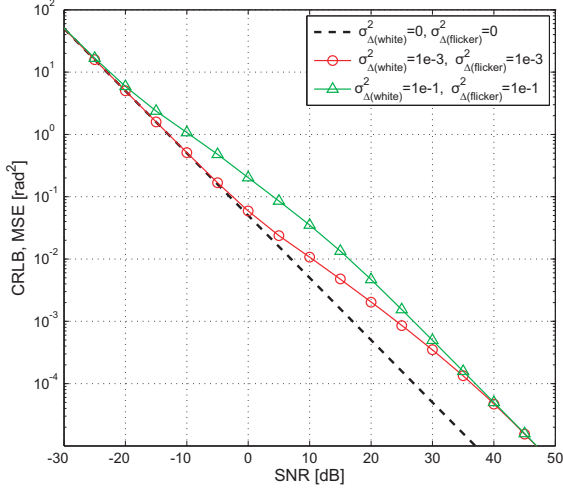
Fig. 6: Comparing CRLBs of NDA method using *slow-varying phase noise* assumption vs. SNR, different phase noise variances. Block length $N = 10$.
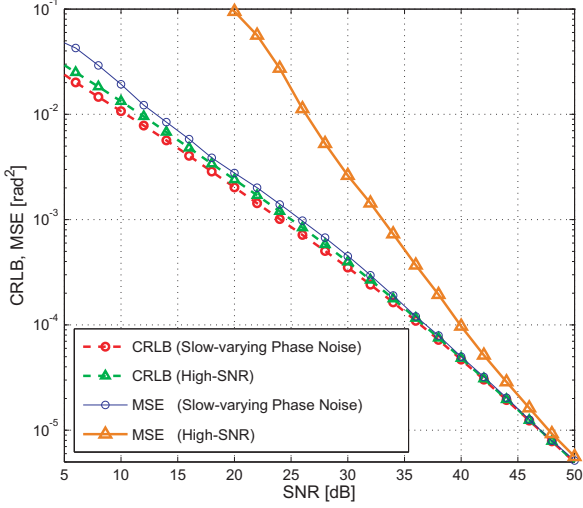

Fig. 7: Comparing performance of NDA method using *High-SNR* assumption vs. *slow-varying phase noise* approach. $\sigma^2_{\Delta_{\text{white}}} = 10^{-3}$, $\sigma^2_{\Delta_{\text{flicker}}} = 10^{-3}$ and block length $N = 10$.
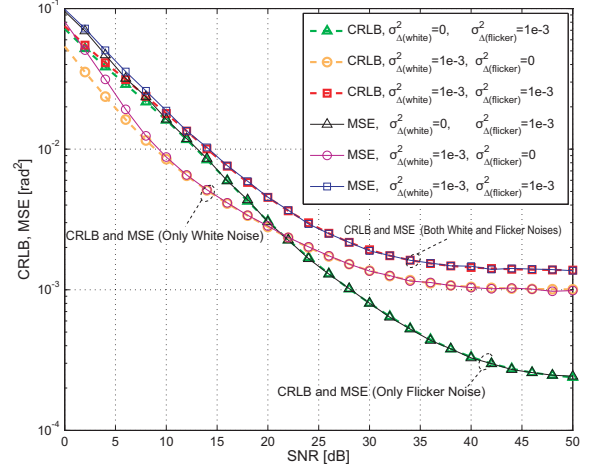

Fig. 8: Comparing CRLBs and estimation MSE of the phase noise caused by white and flicker noise, using DD method with *high-SNR* assumption without data detection error. Block length $N = 10$.
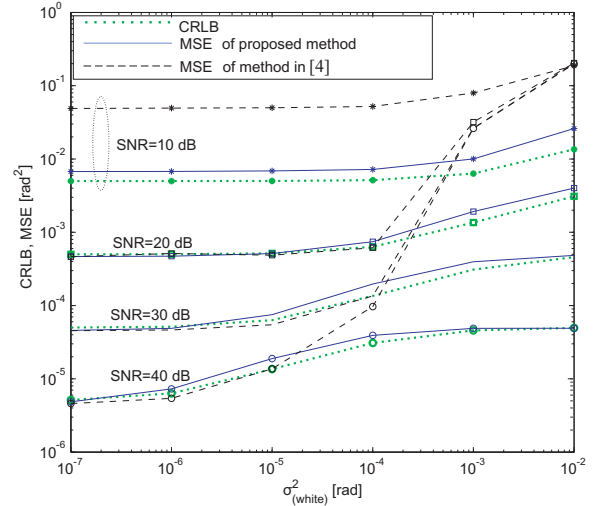

Fig. 9: Comparing the CRLBs and MSEs of *NDA method using slow-varying phase noise assumption* vs. method of [4] for different SNRs, and different white phase noise innovation variances. Block length=11, (Wiener model $\sigma^2_{\Delta_{\text{flicker}}} = 0$).

estimator based on the *slow-varying phase noise* assumption converges to CRLB at low SNR. This is anticipated from the analytical results, since according to (22), for the NDA method, the *high-SNR* assumption is only valid when $M^2 E_s^{(M-1)} \sigma^2_w$ is small. Even with $M = 4$, the results in Fig. 7 show that the assumption in (22) only holds for very high SNR values. In contrast, for the DD estimator, the *high-SNR* assumption is valid when $E_s \sigma^2_w$ is small which is more feasible at moderate SNRs. Thus, performance in this case is independent of the constellation size and it can be seen in Fig. 8 that the DD estimator based on the *high-SNR* approach outperforms the NDA method in Fig. 7. In general, the DD method has an error floor compared with the NDA scheme due to the fact that in the case of DD estimation, only the observation sequence up to the $(k-1)$th symbol is used while estimating the kth symbol's phase noise.

Fig. 8 depicts the performance of the DD method using the *high-SNR* assumption. As it can be seen, in each scenario, the estimator's MSE converges and follows the theoretical CRLB. In this figure, the estimation bounds of phase noise with white and colored innovations are also compared. These results show

that colored phase noise innovations can be more accurately estimated in high SNR. This is anticipated as the correlation between phase innovations can be exploited by the estimator to improve estimation accuracy.

In Fig. 9, the performance of the proposed NDA method using *slow-varying phase noise* approach is compared against the NDA algorithm in [4]. As it can be seen in this figure, the proposed method outperforms the method in [4] for different SNRs and phase noise variances. For slow phase noise variances and high SNRs, the performance of the algorithm in [4] is close to the CRLB. However, unlike the NDA estimators proposed in this paper, for high phase noise variances, the estimator in [4] suffers from an error floor.

VI. CONCLUSIONS

In this paper a new discrete-time model of time-varying phase noise that more closely resembles the measurement results for a free-running oscillator is proposed. Four different NDA and DD MLEs for estimation of the time-varying phase noise are

derived in closed form. The proposed estimators are not based on an exhaustive search and are shown to converge to the CRLBs over a large range of SNR values. In addition, the assumptions that are used in derivation of the bounds and estimators are validated by comparing the results with the available bounds in the literature. It is also shown that the proposed algorithms significantly outperform some of the available estimators.

REFERENCES

[1] N. D'Andrea, U. Mengali, and R. Reggiannini, "Comparison of carrier recovery methods for narrow-band polyphase shift keyed signals," in *Global Telecommunications Conference, 1988, and Exhibition. 'Communications for the Information Age.' Conference Record, GLOBECOM '88., IEEE*, Dec. 1988, pp. 1474 –1478 vol.3.

[2] A. Viterbi, "Nonlinear estimation of psk-modulated carrier phase with application to burst digital transmission," *IEEE Trans. Inf. Theory*, vol. 29, no. 4, pp. 543 – 551, Jul. 1983.

[3] M. Moeneclaey and G. de Jonghe, "ML-oriented NDA carrier synchronization for general rotationally symmetric signal constellations," *IEEE Trans. Commun.*, vol. 42, no. 8, pp. 2531 –2533, Aug. 1994.

[4] H. Meyr, M. Moeneclaey, and S. Fechtel, *Digital Communication Receivers: Synchronization, Channel Estimation, and Signal Processing*. New York, NY, USA: John Wiley & Sons, Inc., 1997.

[5] L. Tomba, "On the effect of wiener phase noise in OFDM systems," *IEEE Trans. Commun.*, vol. 46, no. 5, pp. 580 –583, May 1998.

[6] P. Amblard, J. Brossier, and E. Moisan, "Phase tracking: what do we gain from optimality? particle filtering versus phase-locked loops," *Elsevier Signal Processing*, vol. 83, no. 1, pp. 151 – 167, 2003.

[7] F. Munier, E. Alpman, T. Eriksson, A. Svensson, and H. Zirath, "Estimation of phase noise for QPSK modulation over AWGN channels," *Proc. GigaHertz 2003 Symp.,* Linköping, Sweden, Nov. 2003.

[8] S. Bay, C. Herzet, J.-M. Brossier, J.-P. Barbot, and B. Geller, "Analytic and asymptotic analysis of bayesian cramér rao bound for dynamical phase offset estimation," *IEEE Trans. Signal Process.*, vol. 56, no. 1, pp. 61 –70, jan. 2008.

[9] A. Demir, A. Mehrotra, and J. Roychowdhury, "Phase noise in oscillators: a unifying theory and numerical methods for characterization," *IEEE Trans. Circuits Syst. I, Fundam. Theory Appl.*, vol. 47, no. 5, pp. 655 –674, May 2000.

[10] A. Demir, "Computing timing jitter from phase noise spectra for oscillators and phase-locked loops with white and 1/f noise," *IEEE Trans. Circuits Syst. I, Reg. Papers*, vol. 53, no. 9, pp. 1869 –1884, sept. 2006.

[11] D. Leeson, "A simple model of feedback oscillator noise spectrum," *Proc. IEEE*, vol. 54, no. 2, pp. 329 – 330, Feb. 1966.

[12] J. McNeill, "Jitter in ring oscillators," *IEEE J. Solid-State Circuits*, vol. 32, no. 6, pp. 870 –879, jun 1997.

[13] A. Hajimiri and T. Lee, "A general theory of phase noise in electrical oscillators," *IEEE J. Solid-State Circuits*, vol. 33, no. 2, pp. 179 –194, Feb. 1998.

[14] U. Rohde and A. Poddar, "Noise minimization techniques for RF and MW signal sources," *Microwave Journal*, vol. 50, no. 9, pp. 136 – 162, Sep. 2007.

[15] A. Chorti and M. Brookes, "A spectral model for RF oscillators with power-law phase noise," *IEEE Trans. Circuits Syst. I, Reg. Papers*, vol. 53, no. 9, pp. 1989 –1999, Sep. 2006.

[16] G. Klimovitch, "A nonlinear theory of near-carrier phase noise in free-running oscillators," in *Proc. IEEE Intl. Conf. on Circuits Systs.*, Mar. 2000, pp. 1 –6.

[17] J. Bhatti and M. Moeneclaey, "Feedforward data-aided phase noise estimation from a DCT basis expansion," *EURASIP J. Wirel. Commun. Netw.*, vol. 2009, pp. 4:1–4:11, January 2009.

[18] P. Tichavsky, C. Muravchik, and A. Nehorai, "Posterior cramer-rao bounds for discrete-time nonlinear filtering," *Signal Processing, IEEE Transactions on*, vol. 46, no. 5, pp. 1386 –1396, may 1998.

[19] H. L. V. Trees, *Detection, Estimation and Modulation Theory*. New York: Wiley, 1968,, vol. 1.

[20] J. Dauwels and H.-A. Loeliger, "Phase estimation by message passing," *IEEE Intl. Conf. on Communications*, 2004.

[21] G. Colavolpe, A. Barbieri, and G. Caire, "Algorithms for iterative decoding in the presence of strong phase noise," *IEEE J. Sel. Areas Commun.*, vol. 23, pp. 1748–1757, 2005.

[22] E. Panayrcy, H. Cirpan, and M. Moeneclaey, "A sequential monte carlo method for blind phase noise estimation and data detection," *in Proceedings of the 13th European Signal Processsing Conference (EUSIPCO 05)*, Sep 2005.

[23] F. Herzel, "An analytical model for the power spectral density of a voltage-controlled oscillator and its analogy to the laser linewidth theory," *IEEE Trans. Circuits Syst. I, Fundam. Theory Appl.*, vol. 45, no. 9, pp. 904 –908, Sep. 1998.

[24] G. Niu, "Noise in SiGe HBT RF technology: Physics, modeling, and circuit implications," *Proc. IEEE*, vol. 93, no. 9, pp. 1583 –1597, Sep. 2005.

[25] B. Mandelbrot and J. Van Ness, "Fractional brownian motion, fractional noises and applications," *SIAM Rev.*, vol. 10, no. 4, pp. 422 –437, Oct. 1968.

[26] S. M. Kay, *Fundamentals of Statistical Signal Processing, Estimation Theory*. Prentice Hall, Signal Processing Series, 1993.

[27] F. Munier, T. Eriksson, and A. Svensson, "An ICI reduction scheme for OFDM system with phase noise over fading channels," *IEEE Trans. Commun.*, vol. 56, no. 7, pp. 1119 –1126, Jul. 2008.

[28] T. Schenk, X.-J. Tao, P. Smulders, and E. Fledderus, "On the influence of phase noise induced ici in mimo ofdm systems," *IEEE Commun. Lett.*, vol. 9, no. 8, pp. 682 – 684, aug 2005.

[29] Y. Nasser, M. Des Noes, L. Ros, and G. Jourdain, "On the system level prediction of joint time frequency spreading systems with carrier phase noise," *IEEE Trans. Commun.*, vol. 58, no. 3, pp. 839 –850, march 2010.